Title

Arsenite Binds to ZNF598 to Perturb Ribosome-Associated Protein Quality Control.

Journal

Chemical Research in Toxicology, 33(7)

Authors

Tam, Lok
Jiang, Ji
Wang, Pengcheng
et al.

Publication Date

2020-07-20

DOI

10.1021/acs.chemrestox.9b00412

Peer reviewed

HHS Public Access

Author manuscript

Chem Res Toxicol. Author manuscript; available in PMC 2021 July 20.

Published in final edited form as:

Chem Res Toxicol. 2020 July 20; 33(7): 1644–1652. doi:10.1021/acs.chemrestox.9b00412.

Arsenite Binds to ZNF598 to Perturb Ribosome-Associated Protein Quality Control

Lok Ming Tam,
Environmental Toxicology Graduate Program, University of California, Riverside, California 92521, United States;

Ji Jiang,
Department of Chemistry, University of California, Riverside, California 92521, United States;

Pengcheng Wang,
Department of Chemistry, University of California, Riverside, California 92521, United States

Yinsheng Wang
Environmental Toxicology Graduate Program and Department of Chemistry, University of California, Riverside, California 92521, United States;

Abstract

Arsenic pollution in drinking water is a widespread public health problem, and it affects approximately 200 million people in over 70 countries. Many human diseases, including neurodegenerative disorders, are engendered by the malfunction of proteins involved in important biological processes and are elicited by protein misfolding and/or loss of protein quality control during translation. Arsenic exposure results in proteotoxic stress, though the detailed molecular mechanisms remain poorly understood. Here, we showed that arsenite interacts with ZNF598 protein in cells and exposure of human skin fibroblasts to arsenite results in significant decreases in the ubiquitination levels of lysine residues 138 and 139 in RPS10 and lysine 8 in RPS20, which are regulatory post-translational modifications important in ribosome-associated protein quality control. Furthermore, the arsenite-elicited diminutions in ubiquitinations of RPS10 and RPS20 gave rise to augmented read-through of poly(adenosine)-containing stalling sequences, which was abolished in ZNF598 knockout cells. Together, our study revealed a novel mechanism underlying the arsenic-induced proteostatic stress in human cells.

Graphical Abstract

Corresponding Author: **Yinsheng Wang** - Environmental Toxicology Graduate Program and Department of Chemistry, University of California, Riverside, California 92521, United States; Phone: (951) 827-2700; Yinsheng.Wang@ucr.edu; Fax: (951) 827-4713.

Supporting Information

The Supporting Information is available free of charge at https://pubs.acs.org/doi/10.1021/acs.chemrestox.9b00412.
Transfection efficiencies, ESI-MS/MS, fluorescence microscopy, and images retrieved from FlowJo (PDF).
Complete contact information is available at: https://pubs.acs.org/10.1021/acs.chemrestox.9b00412

The authors declare no competing financial interest.

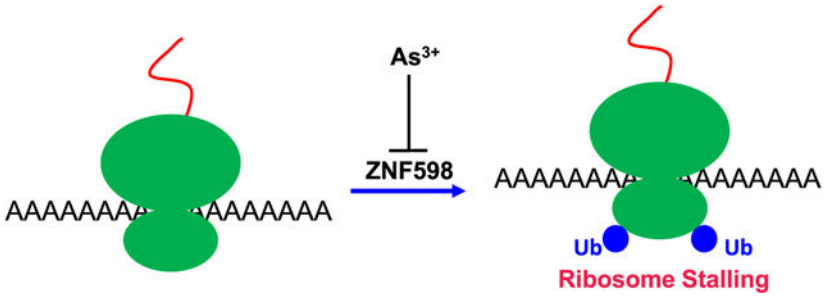

INTRODUCTION

Arsenic is a metalloid prevalent in the environment, where it is naturally present in the Earth's crust and is also anthropogenically introduced to the environment (e.g., through the use of arsenic-containing pesticides).[1,2] Arsenic exists in the environment in inorganic (trivalent arsenite or pentavalent arsenate) or organic forms, where inorganic trivalent arsenite is the most common arsenic species found in the environment and confers the highest potency in toxicity among the different chemical forms of arsenic.[3] Arsenic pollution, which influences more than 200 million people in over 70 countries, is one of the most serious public health problems worldwide.[4] Arsenic exposure contributes to the onset and/or progression of various human diseases, including neurodegenerative disorders, cancers, and type-II diabetes.[5–7] Hence, there is an urgent need for understanding the mechanisms through which arsenic exposure results in human diseases.

Many human diseases can arise from protein misfolding,[8] and chronic exposure to arsenic in human populations can lead to proteotoxic stress.[9] Examples of human diseases emanating from arsenic-induced proteotoxic stress include Alzheimer's disease and Huntington's disease.[8] Epidemiological studies document strong associations between arsenic exposure and cognitive impairment in humans, and animal studies reveal higher incidence of neurodegenerative diseases in rodents treated with arsenic species.[10–12] Therefore, it is important to investigate the mechanisms through which arsenic exposure induces the loss of homeostasis of the proteome (i.e., proteostasis).

Human cells are equipped with multiple mechanisms for maintaining proteostasis, including molecular chaperones, ubiquitin-proteasome system (UPS), and ribosome-associated protein quality control (RQC).[13,14] Among them, RQC is energetically inexpensive, and it promptly eliminates aberrant mRNA and abnormal nascent polypeptides during translation, which constitutes the frontline defense against futile aberrant protein synthesis.[14,15] Poly(adenosine) [Poly(A)] sequences in coding regions of mRNA can result in ribosome stalling and trigger the RQC pathway,[16] which requires regulatory ubiquitinations of RPS10 and RPS20 installed by ZNF598 E3 ubiquitin ligase.[16,17]

Trivalent inorganic arsenic (iAs^{3+}) binds selectively to C_3H- or C_4-type zinc finger proteins (i.e., those with zinc fingers comprised of three cysteines and one histidine, or four cysteines).[18–22] We reasoned that the RING finger motif in ZNF598 may constitute a molecular target for iAs^{3+} binding, and this binding may impair the RQC pathway and

perturb proteostasis.[16,17] In this study, we investigated the interaction between ZNF598 and As^{3+}, examined the iAs^{3+}-induced perturbation in regulatory ubiquitinations of RPS10 and RPS20, and assessed the impact of iAs^{3+} exposure on RQC in human cells.

EXPERIMENTAL PROCEDURES

Cell Culture.

HEK293T cells (ATCC) were cultured in Dulbecco's modified Eagle's medium (DMEM, Thermo Fisher Scientific). HCT-116 cells with the *ZNF598* gene being knocked out and the parental HCT-116 cells were kindly provided by Prof. Eric Bennett from the University of California San Diego,[17] and the cells were also cultured in DMEM. All culture media except those employed for transfection were supplemented with 10% fetal bovine serum (FBS, Thermo Fisher Scientific) and 1% penicillin-streptomycin solution (GE Healthcare). The cells were maintained in a humidified atmosphere with 5% CO_2 at 37 °C, with medium renewal every 2–3 days depending on cell density. For plasmid transfection, the cells were cultured in the same media except that no penicillin-streptomycin solution was added.

Plasmid and Cell Transfection.

The expression plasmid for ZNF598, pcDNA3.1-ZNF598-TEV-3 × Flag, and the reporter cassettes, i.e., pmGFP-P2A-$(K^{AAA})_0$-P2A-RFP and pmGFP-P2A-$(K^{AAA})_{20}$-P2A-RFP, were obtained from Addgene (Cambridge, MA). "P2A" represents the 2A peptide derived from porcine teschovirus-1; ribosomes skip formation of a peptide bond without interrupting translation elongation at P2A sites,[23] which, in the absence of ribosome stalling, allow for equimolar expression of GFP, RFP, and a polypeptide comprised of 20 lysine residues (K20) from the translation of 20 repeats of AAA codon.[16] The expression plasmid for GFP-tagged ZNF598, i.e., pcDNA4/TO-GFP-ZNF598, was kindly provided by Prof. Simon Bekker-Jensen from the University of Copenhagen.[24] The plasmid was transfected into HEK293T cells using TransIT-2020 (Mirus Bio, Madison, WI) according to the manufacturer's protocol.

Streptavidin Agarose Affinity Assay and Western Blot.

The biotin-As probe was previously synthesized.[20] HEK293T cells were transfected with wild-type Flag-ZNF598. At 24 h following the transfection, the cells were exposed with 5 μM biotin-As for 2 h and lysed in CelLytic M lysis buffer supplemented with a protease inhibitor cocktail (Sigma-Aldrich). The cell lysates were subsequently incubated with high-capacity streptavidin agarose beads overnight. The streptavidin agarose beads were then washed with 1× PBS and resuspended in a sodium dodecyl sulfate-polyacrylamide gel electrophoresis (SDS–PAGE) loading buffer.

After SDS–PAGE separation, proteins were transferred to a nitrocellulose membrane using a transfer buffer containing Tris (pH 8.3), methanol, glycine, and water. The membranes were blocked for 1 h with 5% BSA in a 1× PBS-T buffer, which contained PBS and 0.1% (v/v) Tween-20 (pH 7.5) and then incubated with a mouse anti-Flag antibody (1:5000 dilution, Santa Cruz Biotech) at room temperature for 2 h. The membranes were washed with fresh PBS-T at room temperature for 6 times (5–10 min each). After washing, the membranes

were incubated with mouse secondary antibody (1:10000 dilution, Santa Cruz Biotech) at room temperature for 1 h. The membranes were then washed with PBS-T for 6 times. The protein bands were detected by using Amersham ECL Select Western blotting Detection Kit (GE Healthcare) and visualized with Hyblot CL autoradiography film (Denville Scientific, Inc., Metuchen, NJ). Similar experiments were also conducted by pretreating cells with 10 μM $ZnCl_2$, *p*-aminophenylarsine oxide (PAPAO), or $NaAsO_2$ for 1 h prior to the biotin-As treatment.

Stable Isotope Labeling by Amino Acid in Cell Culture (SILAC), As^{3+} Exposure, Immunoprecipitation, and LC–MS/MS Analysis.

SILAC labeling of GM00637 cells in light or heavy RPMI 1640 medium, As^{3+} exposure, immunoprecipitation of ubiquitin remnant peptides, and LC–MS/MS analysis of the enriched peptides were described previously.[25]

Fluorescence Microscopy.

Wild-type pcDNA4/TO-GFP-ZNF598 plasmid (0.5 μg) was transfected into 1×10^5 HEK293T cells seeded on cover glasses placed in a 24-well plate. After 36 h, the transfected cells were mock-treated or treated with 10 μM $ZnCl_2$, $NaAsO_2$, or PAPAO for 2 h and then incubated with 5 μM ReAsH-EDT_2 (Invitrogen, Waltham, MA) in Opti-MEM medium at 37 °C for 1 h. The cells were then washed with 1× BAL buffer three times, fixed with 4% paraformaldehyde for 15 min, and stained with 4′,6-diamidino-2-phenylindole (DAPI). The sample slides were subjected to imaging on a Zeiss 880 confocal microscope with Airyscan (Thornwood, NY) at the wavelengths of 355, 488, and 594 nm for DAPI, GFP, and ReAsH, respectively.

Dual Fluorescence Translation Stalling Assay.

Dual fluorescence reporter plasmids were transfected into cells using TransIT-2020 (Mirus Bio, Madison, WI) following the manufacturer's guidelines. At 24 h following the transfection, the cells were treated with 5.0 μM $NaAsO_2$ (or mock treatment) for another 18 or 24 h. The cells were then subjected to analysis on a MoFlo Astrios EQ Flow Cytometry system (Beckman Coulter, IN), where cellular GFP and RFP fluorescence emissions were measured. The flow cytometry data were analyzed using FlowJo (v9.1).

Statistical Analysis.

Statistical analyses were performed by determining the mean and standard deviation of the values obtained from 3 to 4 independent experiments, except for the fluorescence microscopy data, where images from 30 cells in each group were analyzed, as detailed in the figure legends.

RESULTS

Arsenite Exposure Leads to Decreased Regulatory Ubiquitinations of RPS10 and RPS20.

In this study, we set out to explore whether exposure to inorganic As^{3+} perturbs the RQC pathway by compromising regulatory ubiquitinations involved in this pathway. In this vein,

ubiquitinations of K138 and K139 in RPS10 and that of K8 in RPS20 play an important role in the initiation of ribosome stalling and the onset of the RQC pathway.[16] To this end, we performed a quantitative proteomic experiment, which relies on metabolic labeling using SILAC and immunoprecipitation of tryptic peptides containing diglycine remnant-modified lysine(s), and LC-MS/MS analysis, to identify proteins in GM00637 human skin fibroblasts exhibiting substantial alterations in their ubiquitination levels after a 24 h exposure to 5.0 μM $NaAsO_2$ (Figure 1A).[25] We found that the ubiquitination levels of lysine 138 and 139 (K138 and K139) in RPS10 and K8 in RPS20 were decreased to 60% and 52% of the levels observed in control untreated cells, respectively (Figure 1B). Representative MS and MS/MS results for monitoring the ubiquitination of K8 in RPS20 are shown in Figure 2, and the MS/MS for monitoring the ubiquitinations of K138 and K139 in RPS10 are shown in Figure S1.

Arsenite Binds to the Cysteine Residues in the RING Finger Domain of ZNF598 Protein in Cells.

To further elucidate how arsenite exposure diminishes the regulatory ubiquitinations of RPS10 and RPS20, we focused our attention on ZNF598, the major E3 ubiquitin ligase responsible for these ubiquitinations.[16,17] Along this line, a previous quantitative proteomic study showed that a 24-h treatment of GM00637 cells with 5.0 μM arsenite did not elicit any appreciable changes in the expression level of ZNF598, RPS10, or RPS20 protein, where the corresponding ratios of protein levels in arsenite-treated over mock-treated cells were 0.98 ± 0.07, 1.04 ± 0.08, and 1.03 ± 0.08.[26] Therefore, the arsenite-induced decreases in the levels of ubiquitinated peptides of RPS10 and RPS20 are not due to a diminished expression of these two proteins or ZNF598.

In light of the previous observations about the effects of As(III) binding on modulating the E3 ubiquitin ligase activities of other RING finger proteins,[20–22,25] we reasoned that the decreases in ubiquitination of RPS10 and RPS20 may be attributed to the interaction between As(III) and ZNF598 and the ensuing loss of its E3 ubiquitin ligase activity. To test this, we first examined the interaction between As(III) and ZNF598. We treated HEK293T cells with a *p*-aminophenylarsine oxide-conjugated biotin probe (Figure 3A) and assessed its interaction with ectopically expressed Flag-ZNF598 by a streptavidin agarose affinity assay.[20] The Western blot result revealed that the biotin-As probe facilitated the pull-down of Flag-ZNF598 from human cells, where the control experiment without the addition of the biotin-As probe failed to do so (Figure 3B). In addition, pretreatment of Flag-ZNF598-expressing HEK293T cells with 10 μM PAPAO or $NaAsO_2$, but not $ZnCl_2$, could significantly attenuate the pull-down of Flag-ZNF598 (Figure 3C,D). This result suggests that As^{3+} is capable of displacing the Zn^{2+} ions bound with the RING finger motif of Flag-ZNF598.

We also explored the importance of cysteine residues, located in the RING finger motif of ZNF598, in binding with As^{3+} in cells by utilizing a GFP-tagged ZNF598 expression plasmid and a biarsenical labeling reagent ReAsH-EDT_2, which contains two As^{3+} and displays red fluorescence when four nearby cysteine residues in a protein bind to its arsenic moieties.[22] We observed substantial colocalizations between the ectopically expressed GFP-

ZNF598 and ReAsH in HEK293T cells, suggesting an interaction between As^{3+} and ZNF598 protein in cells (Figure 4 and Figure S2). Moreover, the colocalization between GFP-ZNF598 and ReAsH is markedly attenuated in cells upon pretreatment with PAPAO or $NaAsO_2$, but not Zn^{2+}, supporting the competitive binding of As^{3+} to cysteine residues in the RING finger domain of ZNF598 (Figure 4 and Figure S2).

Arsenite Increases the Ribosomal Read-Through of the $(K^{AAA})_{20}$ mRNA Sequence during Translation.

We next explored the degree to which the As^{3+}-elicited perturbation in ubiquitination of RPS10 and RPS20 affects the RQC pathway. We adopted a previously reported flow cytometry-based assay to assess quantitatively ribosome stalling at poly(A) sites in mammalian cells.[16] In particular, the reporter cassette contains N- and C-terminal GFP and RFP markers flanked by a Flag-tagged stalling reporter (SR, Figure 5A), as described previously.[16] In addition, the open-reading frames of GFP, SR, and RFP are separated by 2A peptide sequence (P2A) derived from porcine teschovirus-1 (Figure 5A). Therefore, translation of the cassette and ribosomal skipping of the P2A sequences yield three proteins (GFP, Flag-SR, and RFP) in equi-molar quantities.[16] In contrast, stalling during translation of Flag-SR would abolish translation prior to RFP synthesis and lead to a substoichiometric RFP/GFP ratio.[16]

Tandem repeats of the AAA lysine codon, i.e., $(K^{AAA})_n$, are among the most potent trigger for ribosome stalling in mammalian cells; thus, the insertion of $(K^{AAA})_n$ in the Flag-SR region can result in an appreciable decrease in the RFP/GFP ratio relative to the reporter lacking the inset between GFP and RFP.[16] Flow cytometry analysis results revealed the expected correlation between GFP and RFP levels across a wide expression range for the cassette with $(K^{AAA})_0$ but significantly reduced RFP for that with $(K^{AAA})_{20}$ (Figure 5C and Figure S3). To explore how arsenite exposure affects the ribosomal stalling of the $(K^{AAA})_{20}$ sequence, we repeated the flow cytometry-based assay for the transfected cells after an 18 h exposure to 5.0 μM As^{3+}. These results show that arsenite exposure led to an increased ratio of RFP/GFP fluorescence intensities (1.26 ± 0.06) when compared to cells without As^{3+} treatment (Figure 5C, Figure S3 and Tables S1–S2), suggesting that arsenite treatment could impede ribosomal stalling during the translation of mRNA sequence containing $(K^{AAA})_{20}$. The enhanced read-through of poly(A) sequence in $(K^{AAA})_{20}$ is also reflected by the scatter plot shown in Figure 5B and Figure S3C. In addition, we examined if the aforementioned effect arises from the As^{3+}-induced augmentation in overall translation elongation by conducting the corresponding experiment with the use of the corresponding reporter cassette without the poly(A) stalling sequence, i.e. $(K^{AAA})_0$. The result showed that arsenite exposure increased the translation of RFP relative to GFP using the $(K^{AAA})_0$ sequence (RFP/GFP = 1.14 ± 0.04), when compared to the cells without As^{3+} treatment (Figure 5C and Figure S3B). After normalization, we found that arsenite exposure augmented the read-through of $(K^{AAA})_{20}$ by 11% (Figure 5D).

Because As^{3+} can also bind to and perturb the functions of other RING finger E3 ubiquitin ligases, we next investigated whether the As^{3+}-promoted read-through of poly(A) mRNA sequence involves the interaction between As^{3+} and ZNF598. For this purpose, we

conducted the same reporter assay by using HCT116 cells with the *ZNF598* gene being knocked out[17] and the parental HCT116 cells (Figure 6, Figures S4–S5 and Tables S1–S2). Our results again revealed that a 24 h exposure of HCT-116 cells to 5.0 μM As^{3+} led to a significant increase (RFP/GFP = 1.23 ± 0.13) in translational read-through of poly(A) mRNA sequence $(K^{AAA})_{20}$ (Figure 6D). This increase, however, was abolished in the isogenic ZNF598 KO cells (Figure 6D). This result, therefore, revealed ZNF598 as an important molecular player contributing to the As^{3+}-induced translational read-through of the poly(A) stalling sequence in the coding region of the template mRNA.

DISCUSSION

As^{3+} Binds to RING Finger Motif of ZNF598 and Induces Proteotoxic Stress.

As^{3+} can interact with zinc finger proteins,[20–22,25,27,28] especially with high affinities to C_3H and C_4 types of zinc fingers.[18] In this study, we provided two lines of evidence to support the notion that arsenite can bind to the RING finger domain of ZNF598 by displacing its bound Zn^{2+} ions. In particular, our results from the confocal fluorescence microscopy experiment with the use of a ReAsH probe and biotin-As pull-down assay revealed the interaction between As^{3+} and ZNF598, which could be pronouncedly weakened by pretreating cells with $NaAsO_2$ or PAPAO, but not with Zn^{2+} (Figures 3–4, Figure S2).

ZNF598 is the major E3 ubiquitin ligase responsible for the regulatory ubiquitinations of ribosomal proteins RPS10 (at K138 and K139) and RPS20 (at K8).[16,17] The RING finger domain of ZNF598 is highly conserved in eukaryotes and is essential for its E3 ubiquitin ligase activity, where the ubiquitin ligase activity of ZNF598 is indispensable for efficient ribosome stalling at poly(A) sequences in coding regions of mRNAs.[29] We found that exposure of cultured human cells to As^{3+} and the ensuing interaction between As^{3+} and ZNF598 led to diminished ubiquitinations of K138 and K139 in RPS10 and K8 in RPS20 (Figures 1–2, Figure S1). We also observed an As(III)-induced augmented translational read-through of the poly(A) stalling sequence in template mRNA in both HEK293T and HCT116 cells and the loss of this effect in HCT116 cells with ZNF598 being genetically ablated (Figures 5–6, Figures S3–S5). In this vein, it is worth noting that arsenite-induced elevation in ribosomal read-through of poly(A) sequence is somewhat modest but statistically significant. These results together substantiate that As^{3+} can displace Zn^{2+} from the RING finger domain of ZNF598, thereby perturbing the RQC pathway.

Disturbance to Protein Quality Control by Arsenic Exposure and Human Diseases.

Proteostasis is maintained by the combined activities of cellular mechanisms regulating protein synthesis, folding, trafficking, degradation, and clearance.[30] RQC constitutes one of the major mechanisms in maintaining proteostasis through strict screening of translation errors; this pathway is initiated by surveillance of defective mRNA, including premature polyadenylated mRNA, followed by degradation of aberrant truncated proteins emanating from stalled ribosomes.[14] In this process, site-specific regulatory ubiquitinations of RPS10 and RPS20 mediated by ZNF598 E3 ubiquitin ligase are required for the detection of ribosomal stalling and triggering the splitting of ribosomal subunits to initiate RQC.[14,29,31]

Arsenic was found to cause protein misfolding and aggregation in yeast and humans,[2,10,32] and arsenite is thought to affect the folding of nascent proteins during translation, though the underlying mechanisms remain unclear.[10] Our findings provided a plausible mechanism about the arsenite-induced perturbation of proteostasis, i.e., through disruption of the ZNF598-mediated RQC pathway. Our observation of modest, yet statistically significant increase of arsenite-induced ribosomal read-through of poly(A) sequence suggests that chronic exposure to arsenic through drinking and ingestion of arsenic-contaminated water may induce translation infidelity. This may constitute a potential mechanism contributing to the pathogenesis of protein misfolding-associated human diseases arising from chronic arsenite exposure.

Implications in Chronic Arsenic Exposure and Risk Assessment for Arsenic-Elicited Human Diseases.

Arsenic pollution, which impacts over 200 million people worldwide via contaminated drinking water and diet, is a serious global public health issue.[4] Chronic arsenic exposure has been associated with many human diseases, ranging from cancer and type-II diabetes to neurodegenerative disorders.[2] Many of these diseases induced by arsenic exposure may originate from loss of proteostasis.[30,33] On the grounds of the adverse health consequences forged by arsenic-induced proteotoxic stress, we should seriously assess and mitigate the risk of chronic arsenic exposure to safeguard public health. This can be achieved by stricter policy regulation on the environmental level of arsenic and improved worldwide public education to raise awareness for remediation of arsenic-contaminated drinking water.[34]

Supplementary Material

Refer to Web version on PubMed Central for supplementary material.

ACKNOWLEDGMENTS

This research was supported by the National Institutes of Health (ES031707 to Y.W.). The authors would like to thank Prof. Eric Bennett at the University of California San Diego and Prof. Simon Bekker-Jensen from the University of Copenhagen for providing important reagents for this research.

REFERENCES

(1). Cholanians AB, Phan AV, Ditzel EJ, Camenisch TD, Lau SS, and Monks TJ (2016) Arsenic induces accumulation of α-synuclein: implications for synucleinopathies and neurodegeneration. Toxicol. Sci 153, 271–281. [PubMed: 27413109]

(2). Chin-Chan M, Navarro-Yepes J, and Quintanilla-Vega B (2015) Environmental pollutants as risk factors for neurodegenerative disorders: Alzheimer and Parkinson diseases. Front. Cell. Neurosci 9, 124. [PubMed: 25914621]

(3). Chen S-J, Zhou G-B, Zhang X-W, Mao J-H, de Thé H, and Chen Z (2011) From an old remedy to a magic bullet: molecular mechanisms underlying the therapeutic effects of arsenic in fighting leukemia. Blood 117, 6425–6437. [PubMed: 21422471]

(4). Ravenscroft P, Brammer H, and Richards K Arsenic Pollution: A Global Synthesis; John Wiley & Sons, 2011; Vol. 94.

(5). Rossman TG, Uddin AN, and Burns FJ (2004) Evidence that arsenite acts as a cocarcinogen in skin cancer. Toxicol. Appl. Pharmacol 198, 394–404. [PubMed: 15276419]

(6). Islam MR, Khan I, Hassan SMN, McEvoy M, D'Este C, Attia J, Peel R, Sultana M, Akter S, and Milton AH (2012) Association between type 2 diabetes and chronic arsenic exposure in drinking water: a cross sectional study in Bangladesh. Environ. Health 11, 38. [PubMed: 22676249]

(7). Chen P, Miah MR, and Aschner M (2016) Metals and neurodegeneration. F1000Research 5, 366.

(8). Chaudhuri TK, and Paul S (2006) Protein-misfolding diseases and chaperone-based therapeutic approaches. FEBS J. 273, 1331–1349. [PubMed: 16689923]

(9). Dodson M, de la Vega MR, Harder B, Castro-Portuguez R, Rodrigues SD, Wong PK, Chapman E, and Zhang DD (2018) Low-level arsenic causes proteotoxic stress and not oxidative stress. Toxicol. Appl. Pharmacol 341, 106–113. [PubMed: 29408041]

(10). Tamas MJ, Sharma SK, Ibstedt S, Jacobson T, and Christen P (2014) Heavy metals and metalloids as a cause for protein misfolding and aggregation. Biomolecules 4, 252–267. [PubMed: 24970215]

(11). O'Bryant SE, Edwards M, Menon CV, Gong G, and Barber R (2011) Long-term low-level arsenic exposure is associated with poorer neuropsychological functioning: a Project FRONTIER study. Int. J. Environ. Res. Public Health 8, 861–874. [PubMed: 21556183]

(12). Escudero-Lourdes C (2016) Toxicity mechanisms of arsenic that are shared with neurodegenerative diseases and cognitive impairment: role of oxidative stress and inflammatory responses. NeuroToxicology 53, 223–235. [PubMed: 26868456]

(13). Valastyan JS, and Lindquist S (2014) Mechanisms of protein-folding diseases at a glance. Dis. Models & Mech 7, 9–14.

(14). Brandman O, and Hegde RS (2016) Ribosome-associated protein quality control. Nat. Struct. Mol. Biol 23, 7–15. [PubMed: 26733220]

(15). Karamyshev AL, and Karamysheva ZN (2018) Lost in translation: Ribosome-associated mRNA and protein quality controls. Front. Genet 9, 431. [PubMed: 30337940]

(16). Juszkiewicz S, and Hegde RS (2017) Initiation of quality control during poly (A) translation requires site-specific ribosome ubiquitination. Mol. Cell 65, 743–750. [PubMed: 28065601]

(17). Sundaramoorthy E, Leonard M, Mak R, Liao J, Fulzele A, and Bennett EJ (2017) ZNF598 and RACK1 regulate mammalian ribosome-associated quality control function by mediating regulatory 40S ribosomal ubiquitylation. Mol. Cell 65, 751–760. [PubMed: 28132843]

(18). Zhou X, Sun X, Cooper KL, Wang F, Liu KJ, and Hudson LG (2011) Arsenite interacts selectively with zinc finger proteins containing C3H1 or C4 motifs. J. Biol. Chem 286, 22855–22863. [PubMed: 21550982]

(19). Zhang X-W, Yan X-J, Zhou Z-R, Yang F-F, Wu Z-Y, Sun H-B, Liang W-X, Song A-X, Lallemand-Breitenbach V, Jeanne M, et al. (2010) Arsenic trioxide controls the fate of the PML-RARα oncoprotein by directly binding PML. Science 328, 240–243. [PubMed: 20378816]

(20). Zhang F, Paramasivam M, Cai Q, Dai X, Wang P, Lin K, Song J, Seidman MM, and Wang Y (2014) Arsenite binds to the RING finger domains of RNF20-RNF40 histone E3 ubiquitin ligase and inhibits DNA double-strand break repair. J. Am. Chem. Soc 136, 12884–12887. [PubMed: 25170678]

(21). Tam LM, Jiang J, Wang P, Li L, Miao W, Dong X, and Wang Y (2017) Arsenite binds to the zinc finger motif of TIP60 histone acetyltransferase and induces its degradation via the 26S proteasome. Chem. Res. Toxicol 30, 1685–1693. [PubMed: 28837777]

(22). Jiang J, Tam LM, Wang P, and Wang Y (2018) Arsenite targets the RING finger domain of Rbx1 E3 ubiquitin ligase to inhibit proteasome-mediated degradation of Nrf2. Chem. Res. Toxicol 31, 380–387. [PubMed: 29658272]

(23). Lin YJ, Huang LH, and Huang CT (2013) Enhancement of heterologous gene expression in Flammulina velutipes using polycistronic vectors containing a viral 2A cleavage sequence. PLoS One 8, e59099. [PubMed: 23516605]

(24). Tollenaere MA, Tiedje C, Rasmussen S, Nielsen JC, Vind AC, Blasius M, Batth TS, Mailand N, Olsen JV, Gaestel M, and Bekker-Jensen S (2019) GIGYF1/2-driven cooperation between ZNF598 and TTP in posttranscriptional regulation of inflammatory signaling. Cell Rep. 26 (3511), 1 DOI: 10.1016/j.celrep.2019.03.006. [PubMed: 30605666]

(25). Jiang J, Bellani M, Li L, Wang P, Seidman MM, and Wang Y (2017) Arsenite binds to the RING finger domain of FANCL E3 ubiquitin ligase and inhibits DNA interstrand crosslink repair. ACS Chem. Biol 12, 1858–1866. [PubMed: 28535027]

(26). Zhang F, Xiao Y, and Wang Y (2017) SILAC-based quantitative proteomic analysis unveils arsenite-induced perturbation of multiple pathways in human skin fibroblast cells. Chem. Res. Toxicol 30, 1006–1014. [PubMed: 28140569]

(27). Shen S, Li X-F, Cullen WR, Weinfeld M, and Le XC (2013) Arsenic binding to proteins. Chem. Rev 113, 7769–7792. [PubMed: 23808632]

(28). Liu S, Jiang J, Li L, Amato NJ, Wang Z, and Wang Y (2015) Arsenite targets the zinc finger domains of Tet proteins and inhibits Tet-mediated oxidation of 5-methylcytosine. Environ. Sci. Technol 49, 11923–11931. [PubMed: 26355596]

(29). Garzia A, Jafarnejad SM, Meyer C, Chapat C, Gogakos T, Morozov P, Amiri M, Shapiro M, Molina H, Tuschl T, et al. (2017) The E3 ubiquitin ligase and RNA-binding protein ZNF598 orchestrates ribosome quality control of premature polyadenylated mRNAs. Nat. Commun 8, 16056. [PubMed: 28685749]

(30). Sweeney P, Park H, Baumann M, Dunlop J, Frydman J, Kopito R, McCampbell A, Leblanc G, Venkateswaran A, Nurmi A, et al. (2017) Protein misfolding in neurodegenerative diseases: implications and strategies. Transl. Neurodegener 6, 6. [PubMed: 28293421]

(31). Joazeiro CA (2017) Ribosomal stalling during translation: providing substrates for ribosome-associated protein quality control. Annu. Rev. Cell Dev. Biol 33, 343–368. [PubMed: 28715909]

(32). Jacobson T, Navarrete C, Sharma SK, Sideri TC, Ibstedt S, Priya S, Grant CM, Christen P, Goloubinoff P, and Tamás MJ (2012) Arsenite interferes with protein folding and triggers formation of protein aggregates in yeast. J. Cell Sci 125, 5073–5083. [PubMed: 22946053]

(33). Kurtishi A, Rosen B, Patil KS, Alves GW, and Møller SG (2019) Cellular proteostasis in neurodegeneration. Mol. Neurobiol 56, 3676–3689. [PubMed: 30182337]

(34). Malik AH, Khan ZM, Mahmood Q, Nasreen S, and Bhatti ZA (2009) Perspectives of low cost arsenic remediation of drinking water in Pakistan and other countries. J. Hazard. Mater 168, 1–12. [PubMed: 19278777]

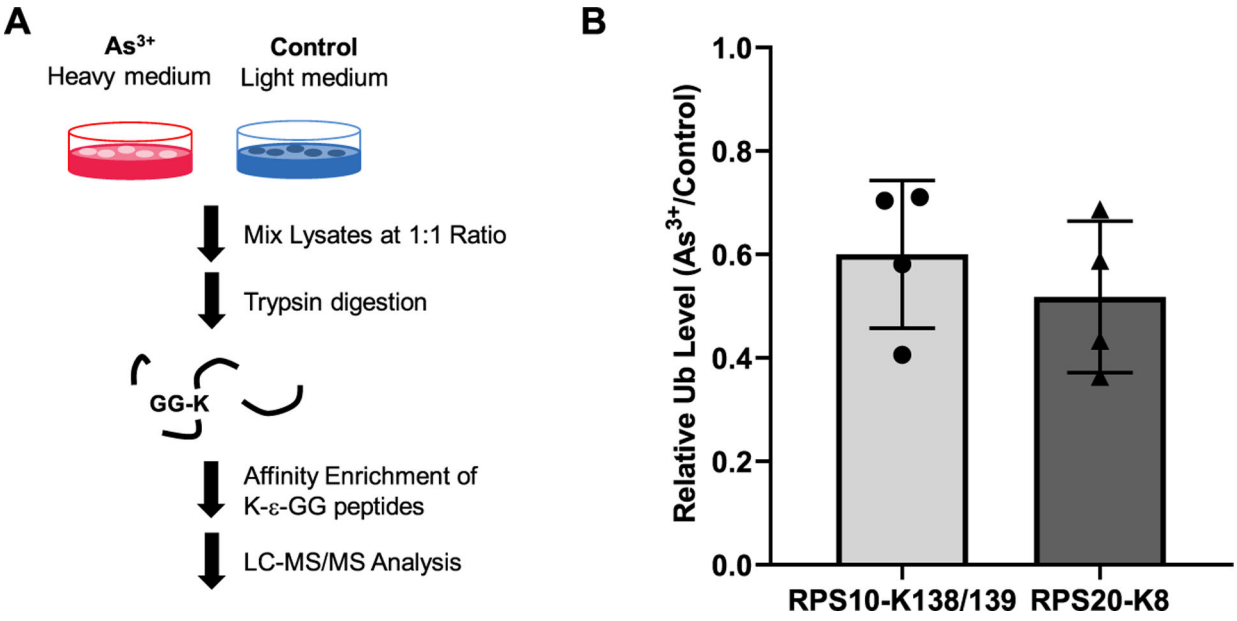

Figure 1.

Arsenite exposure led to diminished levels of site-specific ubiquitinations in ribosomal proteins RPS10 and RPS20. (A) The workflow of SILAC and LC–MS/MS for assessing the effect of a 24 h exposure of GM00637 human skin fibroblast cells to 5 μM $NaAsO_2$ on the global ubiquitinated proteome. (B) Relative ubiquitination levels of K138/K139 in RPS10 and K8 in RPS20 in GM00637 human skin fibroblasts with a 24 h exposure to 5 μM $NaAsO_2$ over the corresponding mock-treated cells (i.e., with water). The relative levels of ubiquitination were determined from the relative abundances of ions observed in ESI-MS for the heavy-/light-labeled (in forward SILAC experiment) or light-/heavy-labeled (in reverse SILAC experiment) diglycine remnant-containing tryptic peptides (Figure 2A). The data represent the mean ± SD of results obtained from 4 biological replicates.

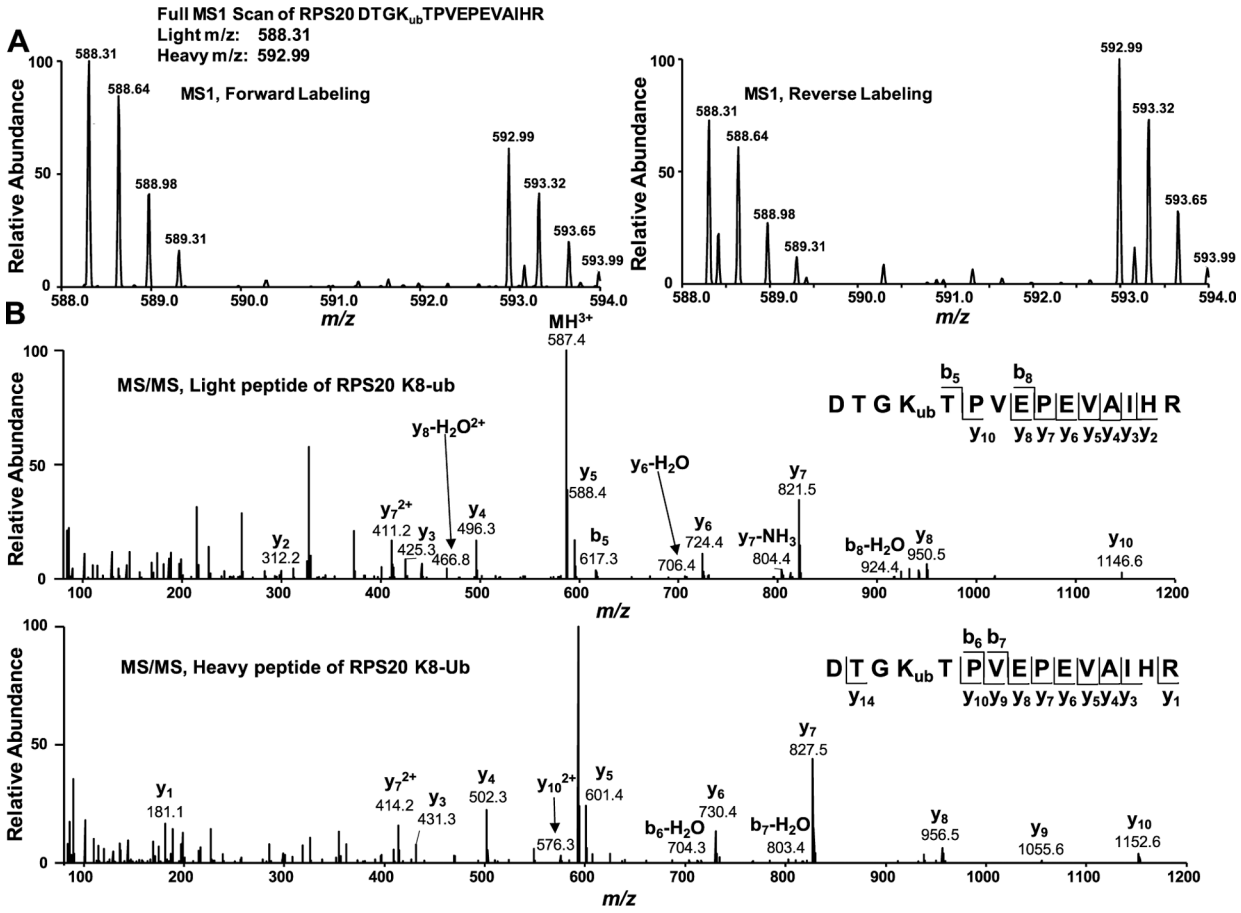

Figure 2.

LC–MS and MS/MS results showing the arsenite-induced decreases in the relative abundance of K-*ε*-GG-containing tryptic peptide, DTG(K8-*ε*-GG)TPVEPEVAIHR, derived from RPS20. (A) Positive-ion ESI-MS showing the $[M + 3H]^{3+}$ ions of the peptide obtained from forward and reverse SILAC experiments, where the *m*/*z* values for the monoisotopic peaks for the light- and heavy-labeled peptide are 588.31 and 592.99, respectively. (B) MS/MS for the light- and heavy-labeled peptide. The insets show schemes summarizing the observed *b* and *y* ions.

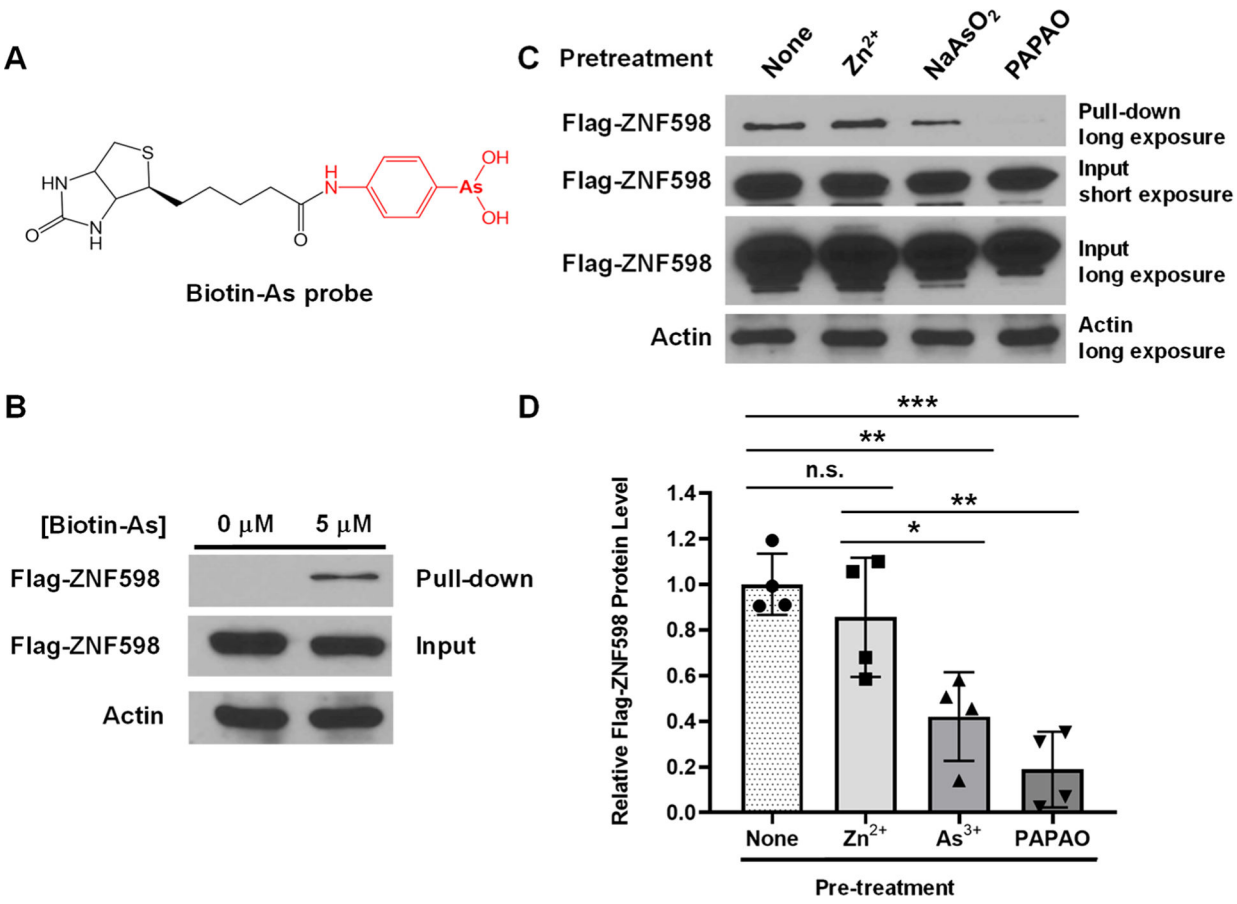

Figure 3.

Biotin-As pull-down assay revealing the interaction between As^{3+} and ZNF598 protein in cells. (A) The chemical structure of the biotin-As probe. (B) Streptavidin agarose affinity pull-down assay showing the interaction between As^{3+} and ZNF598 in cells. The biotin-As probe was used to pull down ectopically expressed Flag-ZNF598 in HEK293T cells. The Flag-ZNF598 in the pull-down sample was probed using the anti-Flag antibody, where Flag-ZNF598 and actin in the input samples were also monitored. The Flag-ZNF598 in the pull-down and input samples were imaged with long and short exposure times, respectively. For comparison, the image for the input lane of Flag-ZNF598 was also acquired with the same (long) exposure time as the pull-down sample. (C, D) The interaction between the biotin-As probe and ZNF598 was substantially diminished upon pretreatment of HEK293T cells with 10 μM $NaAsO_2$ and PAPAO, but not with 10 μM Zn^{2+}. "None" refers to cells without any pretreatment. The Western blot images are shown in (C), and the quantification results are displayed in (D). Relative Flag-ZNF598 protein levels in (D) were determined by dividing the signal of Flag-ZNF598 observed in the pull-down lane with the corresponding signal in the input lane, and the resulting ratios were further normalized against that obtained for the cells without any pretreatment. The data represent mean ± SD of results obtained from 4 biological replicates. The p values were calculated using an unpaired two-tailed Student's t-test (*, $0.01 \leq p < 0.05$; **, $0.001 \leq p < 0.01$; and ***, $p < 0.001$; 'n.s.' stands for no significant difference, i.e., $p > 0.05$).

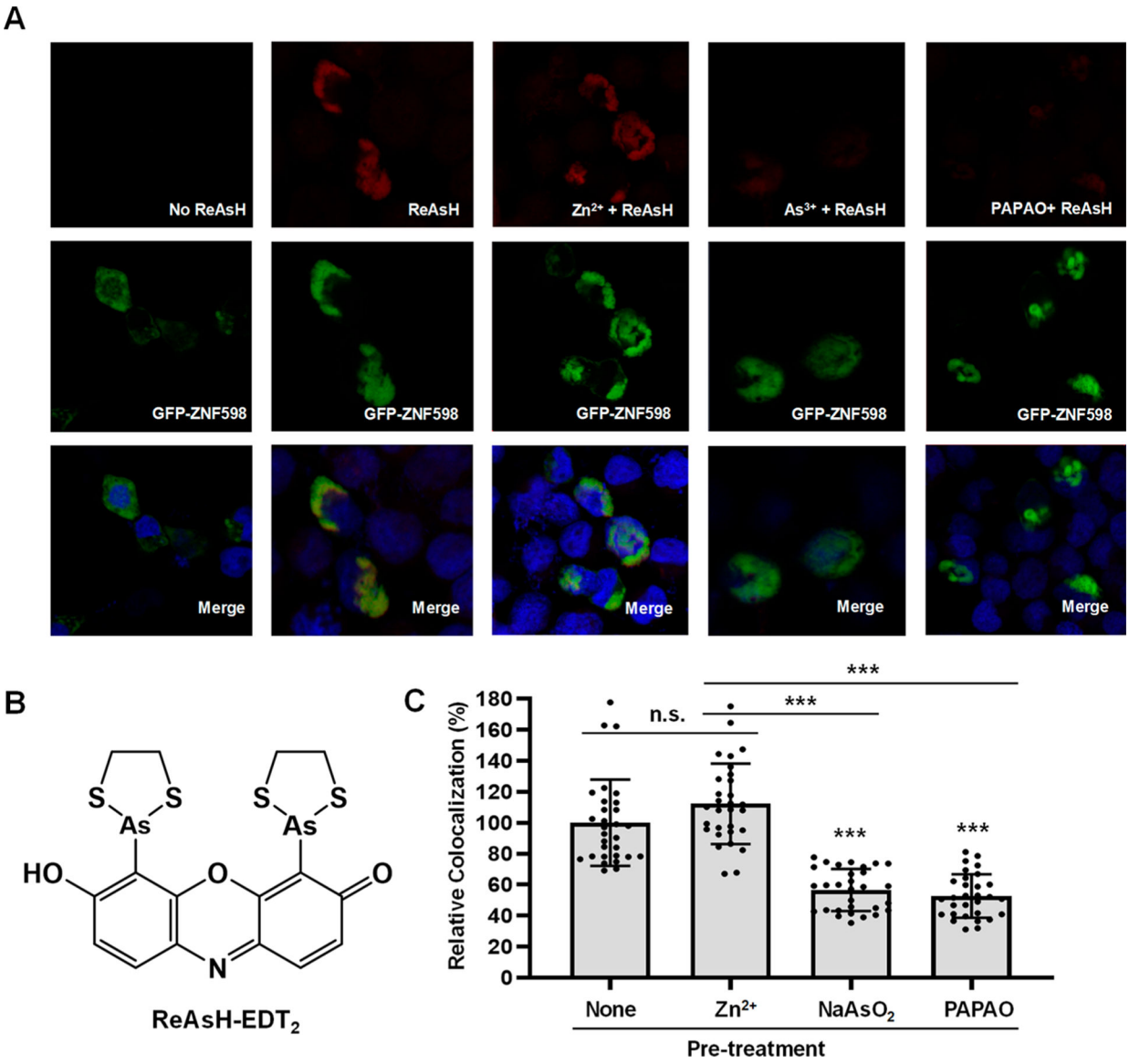

Figure 4.

As^{3+}-bearing ReAsH colocalizes with GFP-ZNF598, and As^{3+} competes with Zn^{2+} for binding to the tetracysteine motif within the RING finger domain of ZNF598. (A) Fluorescence microscopy results revealed the colocalization between ReAsH and ectopically expressed GFP-ZNF598. The colocalization was significantly diminished in cells pretreated with 10 μM $NaAsO_2$ or PAPAO, but not Zn^{2+}. (B) The chemical structure of ReAsH-EDT_2. (C) Quantitative analysis of the frequencies of colocalization between ReAsH-EDT_2 and GFP-ZNF598. The data represent the mean ± SD of results obtained from images of 30 different cells. The p values were calculated using an unpaired two-tailed Student's t-test (*, $0.01 \leq p < 0.05$; **, $0.001 \leq p < 0.01$; and ***, $p < 0.001$; 'n.s.' represents no significant difference, i.e., $p > 0.05$).

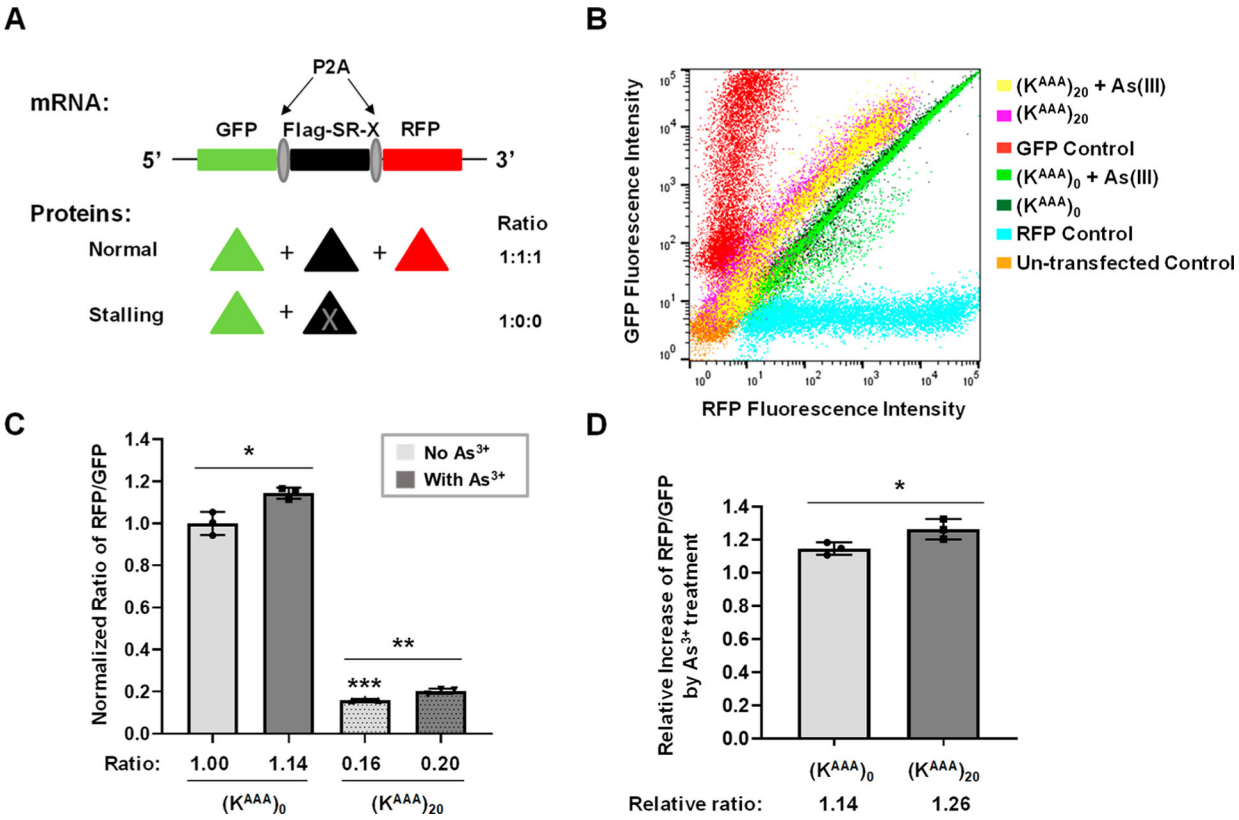

Figure 5.

Arsenite inhibits the ribosomal stalling and augments the read-through of poly(A) stalling sequences. (A) A schematic diagram showing the working principle of the dual fluorescence reporter for monitoring translational stalling at poly(A) sequence in the coding region. Plasmids expressing a reporter without a stall-inducing sequence, i.e. $(K^{AAA})_0$, or one containing 20 consecutive lysine codons $(K^{AAA})_{20}$ in the linker region, was transfected into HEK293T cells. The diagram of the reporter cassette construct and expected protein products in the absence or presence of terminal stalling is modified from the work of Juszkiewicz and Hedge.[16] The reporter cassette contains GFP and RFP flanked by a Flag-tagged stalling reporter (SR), where the open-reading frames GFP, SR, and RFP are separated by 2A peptide sequence (P2A) derived from porcine teschovirus-1. (B) The resulting cellular GFP and RFP levels are depicted in the scatter plot of individual cells. (C) A bar chart showing the RFP/GFP ratios of HEK293T cells transfected with the $(K^{AAA})_0$ or $(K^{AAA})_{20}$ reporter construct in the presence or absence of a 18-hr treatment with 5 μM $NaAsO_2$. The ratios are normalized to that observed for the cells treansfected with $(K^{AAA})_0$ and without $NaAsO_2$ treatment. (D) A bar chart showing the relative ratios of RFP/GFP in arsenite-treated over untreated HEK293T cells transiently expressing the $(K^{AAA})_0$ or $(K^{AAA})_{20}$ reporter. In (C) and (D), the error bars represent SD for three separate transfections and flow cytometry measurements, and the p values were calculated using an unpaired two-tailed Student's t-test (*, $0.01 \leq p < 0.05$; **, $0.001 \leq p < 0.01$; and ***, $p < 0.001$).

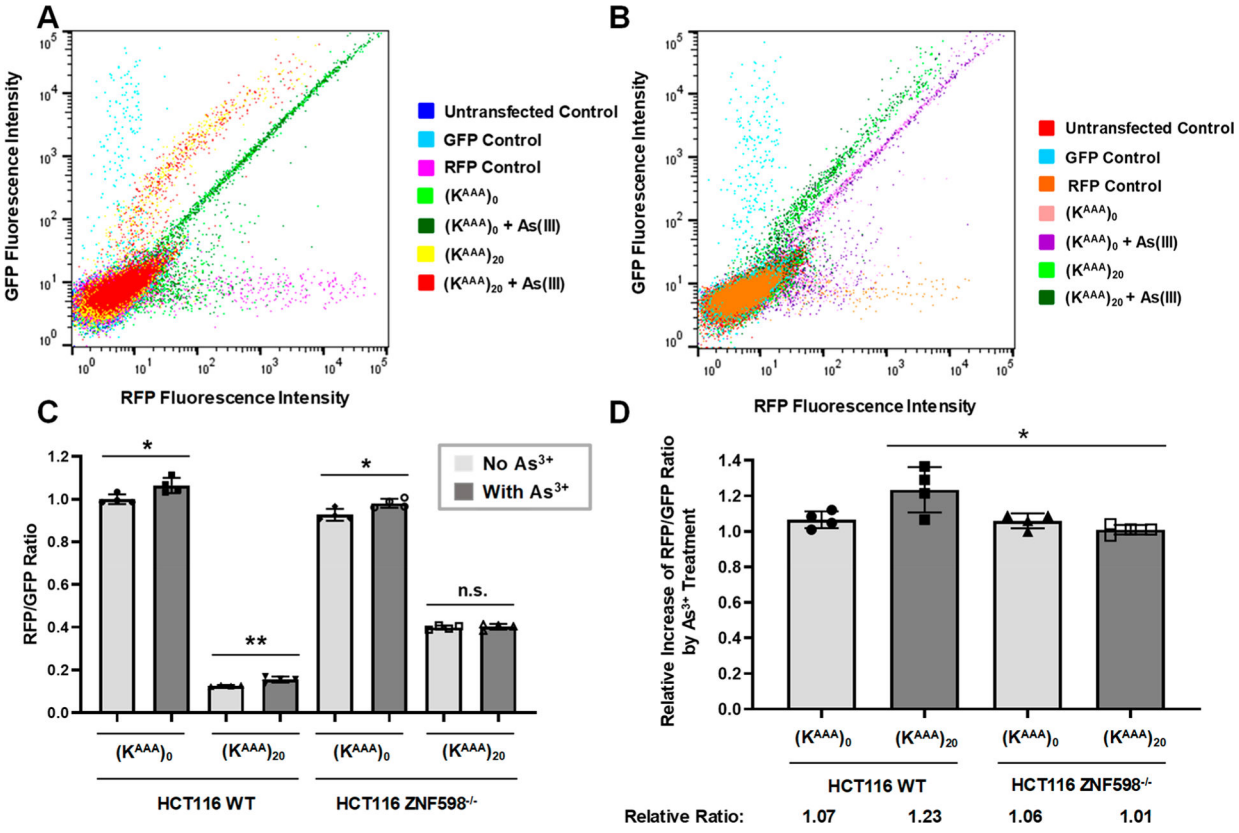

Figure 6.

ZNF598 is the major molecular target of arsenite-elicited increase in ribosomal stalling. (A–B) Scatter plots showing the levels of GFP and RFP in HCT116 cells (A) and the isogenic ZNF598 knockout cells (B). (C) A bar chart indicating the relative RFP/GFP ratio in HCT116 and the isogenic ZNF598 knockout cells transfected with $(K^{AAA})_0$ or $(K^{AAA})_{20}$ dual fluorescence stalling reporter construct, in the presence or absence of 24 h exposure to 5 μM As^{3+}. The ratio is normalized to the ratio of RFP/GFP in wild-type HCT116 cell line transfected with $(K^{AAA})_0$ reporter construct without As^{3+} treatment, which is shown as the control in the diagram. (D) A bar chart showing the relative ratios of RFP/GFP in arsenite-treated over untreated wild-type or *ZNF598*$^{-/-}$ HCT116 cells transfected with $(K^{AAA})_0$ or $(K^{AAA})_{20}$ reporter construct. In (C) and (D), the error bars represent SD for four separate transfections and flow cytometry measurements, and the *p* values were calculated using an unpaired two-tailed Student's *t*-test (*, $0.01 \le p < 0.05$; **, $0.001 \le p < 0.01$; and 'n.s.' represents no significant difference, i.e., $p > 0.05$).